

## Optical conductivity of the Kondo insulator $\text{YbB}_{12}$ : Gap formation and low-energy excitations

H. Okamura

*Department of Physics, Kobe University, Kobe 657-8501, Japan*

S. Kimura

*Graduate School of Science and Technology, Kobe University, Kobe 657-8501, Japan  
and UVSOR Facility, Institute for Molecular Science, Myodaiji, Okazaki 444-8585, Japan*

H. Shinozaki and T. Nanba

*Graduate School of Science and Technology, Kobe University, Kobe 657-8501, Japan*

F. Iga, N. Shimizu, and T. Takabatake

*Graduate School of Advanced Science of Matter, Hiroshima University, Higashi-Hiroshima 739-8526, Japan*

(Received 12 May 1998)

Optical reflectivity experiments have been conducted on single crystals of the Kondo insulator  $\text{YbB}_{12}$  in order to obtain its optical conductivity,  $\sigma(\omega)$ . Upon cooling below 70 K, a strong suppression of  $\sigma(\omega)$  is seen in the far-infrared region, indicating the opening of an energy gap of  $\sim 25$  meV. This gap development is coincident with a rapid decrease in the magnetic susceptibility, which shows that the gap opening has significant influence on magnetic properties. A narrow, asymmetric peak is observed at  $\sim 40$  meV in  $\sigma(\omega)$ , which is attributed to optical transitions between the Yb  $4f$ -derived states across the gap. In addition, a broad peak is observed at  $\sim 0.25$  eV. This peak is attributed to transitions between Yb  $4f$ -derived states and the  $p$ - $d$  band, and is reminiscent of similar peaks previously observed for rare-earth hexaborides. [S0163-1829(98)52236-9]

The term ‘‘Kondo insulators’’, or equivalently ‘‘Kondo semiconductors’’, refers to a group of strongly correlated  $f$ -electron compounds that exhibit the following characteristic behaviors. At high temperatures they behave as Kondo lattice systems with local magnetic moments and are often metallic. In contrast, at low temperatures they become semiconducting as a small energy gap develops at the Fermi energy ( $E_F$ ), and their magnetic susceptibility becomes much smaller.<sup>1,2</sup> While their behaviors have been modeled qualitatively by a hybridization of  $f$  and conduction bands renormalized by correlation effects,<sup>1</sup> the microscopic mechanism for the gap formation is still unclear. In particular, it is not well understood how the local Kondo coupling plays a role in the gap formation. To address these questions, it is important to obtain detailed information about low-energy excitations near  $E_F$ . Optical reflectivity experiments have been useful for this purpose, and have provided much information on Kondo insulators such as  $\text{SmB}_6$  (Refs. 3–5) and  $\text{Ce}_3\text{Bi}_4\text{Pt}_3$ .<sup>6</sup>

Among the Kondo insulators,  $\text{YbB}_{12}$  is the only known Yb-based compound, and it has been studied extensively.<sup>7–9</sup> The magnetic susceptibility of  $\text{YbB}_{12}$  shows a Curie-Weiss behavior at high temperatures, but it decreases rapidly upon cooling below  $\sim 70$  K. The presence of an energy gap has been shown by activation-type temperature dependences in dc resistivity, specific heat, and Hall effect measurements, with measured gap  $2\Delta$  in the range 10–15 meV.<sup>7</sup> Previously, only sintered, polycrystalline samples were available due to difficulties in crystal growth, which limited a reliable optical measurement to the far-infrared.<sup>8</sup> Recently, however, Iga *et al.*<sup>10</sup> have successfully grown large single crystals of  $\text{YbB}_{12}$  and other rare-earth dodecaborides.

In this work, we report the first optical reflectivity measurements of single crystals  $\text{YbB}_{12}$ , at photon energies between 0.008 eV and 50 eV and at temperatures between 20 K and room temperature. The resulting optical conductivity spectrum  $\sigma(\omega)$  has revealed many optical transitions that were previously unknown. Below 70 K,  $\sigma(\omega)$  clearly shows the formation of an energy gap of  $\sim 25$  meV. This gap opening is coincident with a rapid decrease in the magnetic susceptibility, showing that the gap opening has large effects on the magnetic properties. Other low-energy excitations are analyzed in terms of the  $f$ - and the  $pd$ -derived states near  $E_F$ . We have also studied single crystals of  $\text{LuB}_{12}$ , which is a non-magnetic metal with a filled  $4f$  shell, for comparison to  $\text{YbB}_{12}$ .

Single crystals of  $\text{YbB}_{12}$  and  $\text{LuB}_{12}$  were grown by the floating-zone method using a newly developed image furnace equipped with four Xe lamps.<sup>10</sup> Both compounds have a cubic, NaCl-type structure consisting of Yb or Lu ions and  $\text{B}_{12}$  cubo-octahedrons. The samples, with typical dimensions of  $\sim 6$  mm diam and  $\sim 1$  mm thickness, were polished and mounted on a liquid He cryostat, which was inserted into a vacuum chamber that contained the necessary optics for reflectivity measurements under near-normal incidence. An evaporated Au or Al film was mounted next to the samples as a reference mirror. For measurements below 2.5 eV, a rapid-scan Fourier interferometer (Bruker Inc. IFS-66v) was used with various combinations of beam splitters, detectors and light sources, including synchrotron radiation at beamline BL6A1 of the UVSOR Facility, Institute for Molecular Science.<sup>11</sup> Measurements between 2 and 50 eV were performed at room temperature only, using synchrotron radiation at beamlines BL1B and BL5B of UVSOR. The reflec-

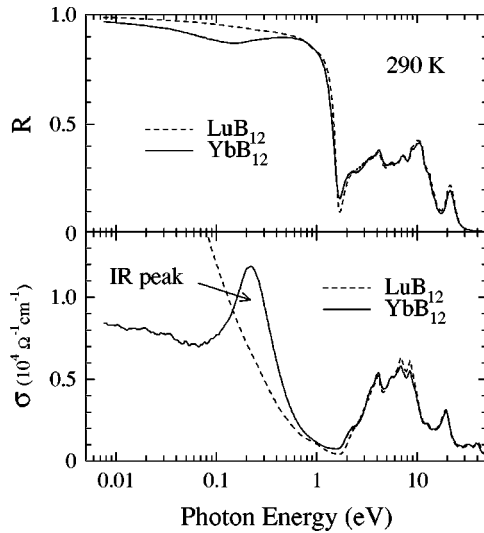


FIG. 1. Reflectivity ( $R$ ) and optical conductivity ( $\sigma$ ) spectra of  $\text{YbB}_{12}$  and  $\text{LuB}_{12}$  single crystals at 290 K.

tivity of the samples was also checked using He-Ne and Ar lasers at several photon energies. Standard Kramers-Kronig analyses were made to obtain  $\sigma(\omega)$  from a measured reflectivity spectrum  $R(\omega)$ , combined with a Hagen-Rubens extrapolation [ $R(\omega) \propto 1 - a\sqrt{\omega}$ ] to the lower-energy end and a  $R(\omega) \propto \omega^{-4}$  extrapolation for the higher-energy end.<sup>12</sup>

Figure 1 shows  $R(\omega)$  and  $\sigma(\omega)$  of  $\text{YbB}_{12}$  and  $\text{LuB}_{12}$  single crystals at room temperature. For both compounds, a sharp onset is seen in  $R(\omega)$  near 1.6 eV, which can be identified as the plasma edge ( $\omega_p$ ) due to a metallic response of mobile carriers. The peak structures above  $\omega_p$  are due to interband transitions between electronic states far apart from  $E_F$ .<sup>13</sup> The similarity of these spectra above  $\omega_p$  for  $\text{YbB}_{12}$  and  $\text{LuB}_{12}$  shows that these states are nearly unaffected by Yb/Lu replacement. Below  $\omega_p$ , in contrast, the spectra are strikingly different for the two compounds: In  $\text{LuB}_{12}$ ,  $R(\omega)$  is nearly flat and  $\sigma(\omega)$  shows a sharp rise, which is typical of a good metal, while in  $\text{YbB}_{12}$  there is a broad dip in  $R(\omega)$  giving rise to a strong peak at 0.25 eV in  $\sigma(\omega)$ . Hereafter we refer to this peak as the “IR peak”, and concentrate on the spectra below  $\omega_p$ . Detailed analyses on the interband transition peaks above  $\omega_p$  will be presented elsewhere.<sup>14</sup>

Figure 2 shows  $R(\omega)$  and  $\sigma(\omega)$  for  $\text{YbB}_{12}$  measured at 290, 160, 78, and 20 K. As the temperature is lowered from 290 K to 78 K,  $\sigma(\omega)$  is gradually reduced over the entire infrared region, and the IR peak becomes enhanced and slightly blueshifted. At 78 K the spectra are still metallic, in the sense that  $R(\omega)$  approaches 1 at the lower energy end. At 20 K, however, the spectral weight below  $\sim 40$  meV in  $\sigma(\omega)$  is strongly depleted; the spectrum is now typical of an insulator (semiconductor) with an energy gap. Note that, on cooling from 78 K to 20 K, the spectral weight lost by the gap formation in  $\sigma(\omega)$  is transferred to the higher-energy side of the IR peak. Namely, the optical sum rule is satisfied by transfers of spectral weight over an energy scale of  $\sim 1$  eV, rather than by transfers to directly above the gap. This point will be discussed later. The temperature dependence of  $R(\omega)$  and  $\sigma(\omega)$  below 78 K is shown in Fig. 3 for the low-energy region. These spectra demonstrate that the gap develops progressively over the temperature range  $T \leq 70$  K. At 20 K the

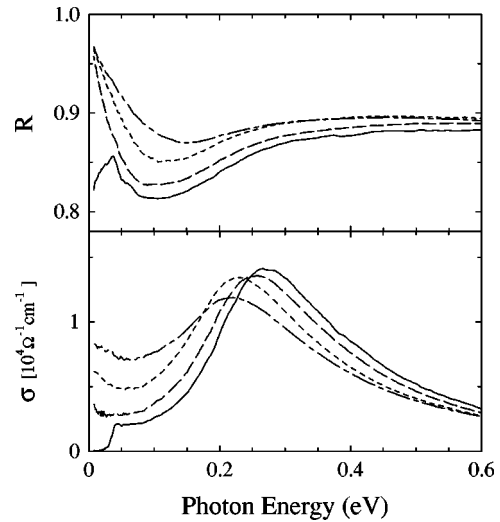


FIG. 2. Reflectivity ( $R$ ) and optical conductivity ( $\sigma$ ) of  $\text{YbB}_{12}$  in the infrared region at 290 K (dotted-dashed curve), 160 K (dotted), 78 K (dashed), and 20 K (solid).

gap appears fully developed, with an “onset” of  $\sigma(\omega)$  at  $\sim 25$  meV. Above the onset,  $\sigma(\omega)$  rises quickly to a “shoulder” at  $\sim 40$  meV, which is marked by the arrow in Fig. 3. Since the spectral weight below the onset is very small, we identify the onset energy as the magnitude of the gap,  $2\Delta_{opt} \approx 25$  meV.

There are remarkable aspects in the temperature dependence and the magnitude of the observed gap in  $\sigma(\omega)$ . The inset of Fig. 3 shows  $\chi(T)$ , the magnetic susceptibility of the single crystal  $\text{YbB}_{12}$  as a function of temperature.<sup>10</sup>  $\chi(T)$  has a broad maximum at  $T_{max} \sim 75$  K. Below  $T_{max}$  it decreases rapidly with cooling, and results in a finite value at low temperatures.<sup>2,15</sup> Comparing the optical spectra in Fig. 3 with

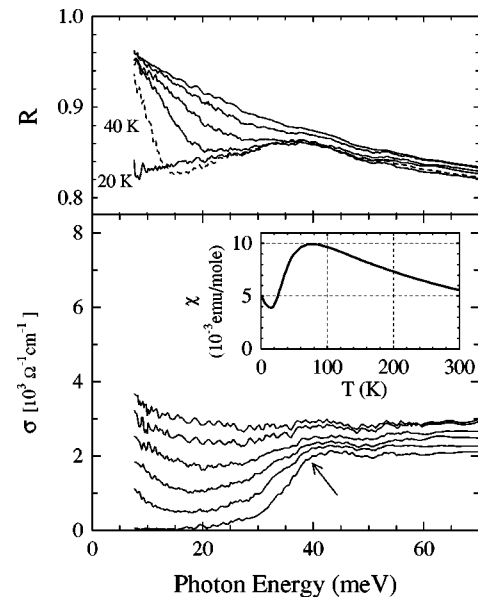


FIG. 3. Reflectivity ( $R$ ) and optical conductivity ( $\sigma$ ) of  $\text{YbB}_{12}$  at, from top to bottom curves for both  $R$  and  $\sigma$ ,  $T = 78, 70, 60, 50, 40,$  and  $20$  K. The arrow indicates the “shoulder” discussed in the text. The inset shows the magnetic susceptibility ( $\chi$ ) of  $\text{YbB}_{12}$  single crystal as a function of temperature ( $T$ ).

$\chi(T)$ , it is clear that the gap development coincides with the rapid decrease of  $\chi(T)$  in exactly the same temperature range. Although it is very likely that the gap opening and the decrease in  $\chi$  are closely related to each other,<sup>2</sup> the microscopic mechanism connecting them is not well understood yet. At higher temperatures where the gap is not fully developed, the  $f$  and conduction electrons may form local ‘‘Kondo singlets’’, resulting in a reduction in  $\chi$  as observed.<sup>6</sup> On the other hand, the large residual  $\chi$  at low temperatures is suggestive of a Van Vleck-type paramagnetism,<sup>2,15</sup> which may arise from excited states above the gap.

Another remarkable aspect is that the gap magnitude  $2\Delta_{opt}$  is much greater than the transport gap measured by the dc resistivity,  $2\Delta_\rho \approx 12$  meV.<sup>10</sup> In addition, the temperature below which the gap appears in  $\sigma(\omega)$  is much lower than  $\Delta_{opt}/k_B \approx 145$  K. These behaviors are unexpected for thermal activation of carriers across a conventional, direct band gap, since in such a case  $2\Delta_{opt}$  should be close to  $2\Delta_\rho$ , and the gap should appear in  $\sigma(\omega)$  at  $T \sim \Delta_{opt}/k_B$ . However, if the dispersion near  $E_F$  does not form a direct gap,  $2\Delta_{opt}$  is not necessarily equal to  $2\Delta_\rho$ . Mutou and Hirashima<sup>16</sup> performed numerical calculations based on the periodic Anderson model in infinite dimensions to analyze the temperature-dependent properties of Kondo insulators. They showed that  $\Delta_{opt} \approx 2\Delta_\rho$ , and that the gap appears in  $\sigma(\omega)$  at  $T \approx (1/2)\Delta_{opt}/k_B$ , not at  $\Delta_{opt}/k_B$ . Similar results were given independently by Rozenberg *et al.*<sup>17</sup> These behaviors arise from an *indirect* gap formed by the hybridization of narrow  $f$  and broad conduction bands renormalized by strong correlation effects. Since  $\sigma(\omega)$  mainly probes the oscillator strength and the density of states (DOS) for direct ( $k$ -conserving) transitions,  $2\Delta_{opt}$  is generally larger than  $2\Delta_\rho$  if the gap in the total (both direct and indirect) DOS is indirect. They also showed that the temperature range for the gap development in  $\sigma(\omega)$  is nearly the same as that for the decrease in  $\chi(T)$ . These theoretical predictions are in good agreement with the present experimental results.

These characteristic behaviors of the energy gap in  $\sigma(\omega)$  and the coincidence of gap formation with a decrease in  $\chi$  are very similar to the results for the Ce-based Kondo insulator  $\text{Ce}_3\text{Bi}_4\text{Pt}_3$ .<sup>6</sup> Since these behaviors are shared by the two representative Kondo insulators, they are likely to be universal optical features of Kondo insulators. A difference is seen, however, in the spectral shape of the gap in  $\sigma(\omega)$ : For  $\text{YbB}_{12}$  the spectral weight within the gap is very weak at low temperatures, as seen in Fig. 3. In contrast, for  $\text{Ce}_3\text{Bi}_4\text{Pt}_3$  the spectral depletion within the gap is weaker, with a large ‘‘tail’’ persisting down to the low-energy end of  $\sigma(\omega)$ .<sup>6</sup>

Now we attempt to analyze the low-energy excitations above the gap, in particular the shoulder at 40 meV and the IR peak at 0.25 eV. As shown in Fig. 4(a), the IR peak can be fitted well by the classical Lorentz oscillator model<sup>18</sup>

$$\sigma_L(\omega) \propto \frac{\Gamma \omega^2}{(\omega^2 - \omega_0^2)^2 + \Gamma^2 \omega^2}, \quad (1)$$

where  $\omega_0$  is the peak energy and  $\Gamma$  is the peak width. In order to separate the shoulder and the IR peak, we fitted the IR peak at each temperature using (1), then subtracted the fitting function from  $\sigma(\omega)$ . The resulting (subtracted) spectra at 78, 50, and 20 K are shown in Fig. 4(b). These spectra

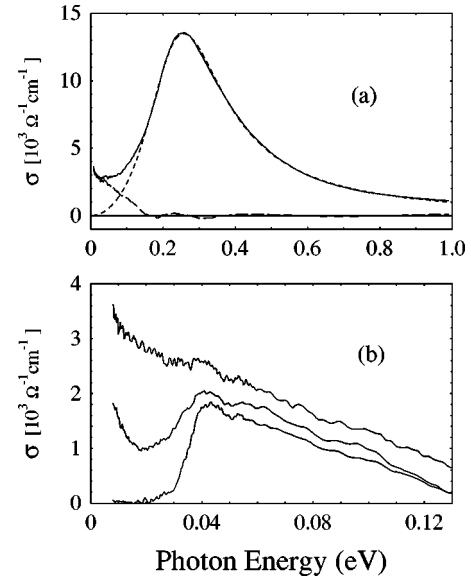


FIG. 4. (a) Optical conductivity of  $\text{YbB}_{12}$  at 78 K (solid curve), a fitting based on (1) (dotted), and the resulting spectrum (dashed) obtained after the subtraction. (b) The resulting spectra obtained after the fitting-subtraction procedure at (top to bottom) 78, 50, and 20 K.

reveal that the shoulder is actually an asymmetric *peak*. We attribute this peak to electronic excitations across the gap, from mainly Yb  $4f$ -derived states below  $E_F$  to those above  $E_F$ . Note that a  $4f$ - $4f$  transition is optically forbidden, but mixing with other symmetry states (e.g., Yb  $5d$ ) may make the transition partially allowed. This interpretation is consistent with theoretical calculations<sup>16,17,19</sup> and photoemission (PE) experiment.<sup>9</sup> Band calculations<sup>19</sup> for  $\text{YbB}_{12}$  show a large Yb  $4f$ -derived DOS below and above  $E_F$ , and numerical calculations based on the periodic Anderson model also showed large  $f$ -derived DOS below and above the Kondo insulating gap.<sup>16,17</sup> PE experiments<sup>9</sup> of  $\text{YbB}_{12}$  found a narrow, asymmetric peak located  $\sim 25$  meV below  $E_F$ , which was mainly due to the Yb  $4f$ -derived DOS. Since  $\sigma(\omega)$  probes direct transitions between occupied and unoccupied states, we cannot simply compare  $\sigma(\omega)$  with the PE spectrum, which probes the total DOS for the occupied states only. Nevertheless, the position of the gap excitation peak in  $\sigma(\omega)$ , 40 meV, is comparable with the peak in the PE spectrum, assuming that  $E_F$  is located near the middle of the gap.

The IR peak is observed for  $\text{YbB}_{12}$ , but not for  $\text{LuB}_{12}$ , as shown in Fig. 1. The most significant difference in the electronic states of these two compounds is the position of  $4f$ -derived states: There is a large Yb  $4f$ -derived DOS near  $E_F$  in  $\text{YbB}_{12}$  while Lu  $4f$ -derived states in  $\text{LuB}_{12}$  are located  $\sim 5$  eV below  $E_F$ .<sup>9,19</sup> Therefore, the IR peak is likely to be related to Yb  $4f$ -derived states near  $E_F$ . We tentatively attribute the IR peak to optical transitions between the Yb  $4f$ -derived narrow band near  $E_F$  and the broad conduction band, which mainly consists of B  $2p$ - and Yb  $5d$ -derived states.<sup>19</sup> Both transitions from the  $4f$  band below  $E_F$  to the  $p$ - $d$  band above  $E_F$  and those from  $p$ - $d$  below  $E_F$  to  $4f$  above  $E_F$  are possible. The much larger integrated strength and the much larger width of the IR peak than the gap excitation peak supports this assignment, since an  $f$ - $d$  transition is optically allowed and the  $p$ - $d$  bands are much broader

than the  $f$  band. Also, the involvement of the Yb  $4f$ -derived states near  $E_F$  in *both the gap excitation peak and the IR peak* is consistent with the observation that the spectral weight lost in  $\sigma(\omega)$  by the gap formation is distributed over a wide energy range ( $\sim 1$  eV) covering the entire IR peak, rather than distributed to a narrow energy range directly above the gap.

Anomalous infrared absorption similar to the IR peak for YbB<sub>12</sub> has been also observed for rare-earth hexaborides (RB<sub>6</sub>'s) with partially-filled  $4f$  shells, including SmB<sub>6</sub>, CeB<sub>6</sub>, and others.<sup>5</sup> The intensity of the observed infrared absorption in RB<sub>6</sub>'s with different  $R$  elements was found to be proportional to the number of  $4f$  electrons, and the absorption was attributed to an indirect  $d$ - $d$  transition assisted by exchange scattering.<sup>5</sup> Such specific assignment for the IR peak is beyond the scope of the present work, and other RB<sub>12</sub>'s with different  $R$  elements must be studied and compared to better understand the nature of the IR peak.

In conclusion, we have reported the first optical reflectivity experiment on single crystal YbB<sub>12</sub>. An energy gap for-

mation was clearly observed in  $\sigma(\omega)$  below  $\sim 70$  K. The gap opening was coincident with a large reduction of magnetic susceptibility, showing that the gap formation affects the magnetic properties significantly. The temperature dependence and the magnitude of the gap in  $\sigma(\omega)$  showed anomalous behaviors, which are probably characteristic of Kondo insulators as predicted theoretically. Two prominent low-energy excitation peaks were observed, which were attributed to  $f$ - $f$  and  $f$ - $pd$  transitions.

We would like to thank H. Harima for providing unpublished band calculations of YbB<sub>12</sub>, LuB<sub>12</sub>, and YB<sub>12</sub>. H.O. thanks T. Mutou for many stimulating discussions and for providing unpublished simulations on Kondo insulators. We acknowledge financial support from the REIMEI Research Resources, the Atomic Energy Research Institute, the Electric Technology Research Foundation of Chugoku, and the Grants-in-Aid from the Ministry of Education, Science and Culture.

- 
- <sup>1</sup>G. Aeppli and Z. Fisk, *Comments Condens. Matter Phys.* **16**, 155 (1992).
- <sup>2</sup>T. Takabatake *et al.*, *J. Magn. Magn. Mater.* **177–181**, 277 (1998).
- <sup>3</sup>G. Travaglini and P. Wachter, *Phys. Rev. B* **29**, 893 (1984).
- <sup>4</sup>T. Nanba *et al.*, *Physica B* **186–188**, 440 (1993).
- <sup>5</sup>S. Kimura, T. Nanba, S. Kunii, and T. Kasuya, *Phys. Rev. B* **50**, 1406 (1994).
- <sup>6</sup>B. Bucher, Z. Schlesinger, P. C. Canfield, and Z. Fisk, *Phys. Rev. Lett.* **72**, 522 (1994).
- <sup>7</sup>M. Kasaya *et al.*, *J. Magn. Magn. Mater.* **31–34**, 438 (1983); **47&48**, 429 (1985); F. Iga, M. Kasaya, and T. Kasuya, *ibid.*, **52**, 279 (1985); **76&77**, 156 (1988).
- <sup>8</sup>P. Wachter and G. Travaglini, *J. Magn. Magn. Mater.* **47&48**, 423 (1985).
- <sup>9</sup>T. Susaki *et al.*, *Phys. Rev. Lett.* **77**, 4269 (1996); *Phys. Rev. B* **56**, 13 727 (1997).
- <sup>10</sup>F. Iga, N. Shimizu, and T. Takabatake, *J. Magn. Magn. Mater.* **177–181**, 337 (1998).
- <sup>11</sup>M. Sakurai *et al.*, *J. Synchrotron Radiat.* **5**, 578 (1998).
- <sup>12</sup>The result of a Hagen-Rubens extrapolation was examined by comparing the extrapolated  $\sigma(\omega)$  with the measured dc conductivity.
- <sup>13</sup>S. Kimura *et al.*, *Phys. Rev. B* **46**, 12 196 (1992).
- <sup>14</sup>S. Kimura *et al.* (unpublished).
- <sup>15</sup>The small rise in  $\chi(T)$  seen for  $T \leq 15$  K is due to residual impurities (Refs. 2 and 10). For more recently grown single crystals with less impurities, this rise is much weaker, but there still remains a large, nearly temperature-independent susceptibility,  $\chi \sim 3.2 \times 10^{-3}$  emu/mol. [F. Iga *et al.* *Physica B* (to be published)].
- <sup>16</sup>T. Mutou and D. Hirashima, *J. Phys. Soc. Jpn.* **63**, 4475 (1994); **64**, 4799 (1995).
- <sup>17</sup>M. J. Rozenberg, G. Kotliar, and H. Kajueter, *Phys. Rev. B* **54**, 8452 (1996).
- <sup>18</sup>F. Wooten, *Optical Properties of Solids* (Academic Press, New York, 1972).
- <sup>19</sup>H. Harima, A. Yanase and T. Kasuya, *J. Magn. Magn. Mater.* **47&48**, 567 (1985); A. Yanase and H. Harima, *Prog. Theor. Phys. Suppl.* **108**, 19 (1992); H. Harima (unpublished).